Proc. of the Second Intl. Conf. on Advances In Civil, Structural and Mechanical Engineering- CSM 2014.

ISBN: 978-1-63248-054-5 doi: 10.15224/ 978-1-63248-054-5-114

Design and Experimental Tests of a Mechatronic Device for both Active Vibration and Motion Control

Paolo Righettini, Roberto Strada, Riccardo Riva

***Abstract*— This paper deals with the mechatronic design of an active device for both the control of vibration and the trim's regulation. In particular, the design concerns a 3 dof actuated device which controls vibrations and trim of a platform. A detailed model of the system has been developed, also identifying some unknown parameters by means of specific experimental tests. The detailed model of the system allowed to set-up an effective control system able also to compensate friction. After the design phase, several experimental tests have been performed, in order to evaluate the performances of the control strategy chosen**

***Keywords*—active vibration control, motion control, experimental tests**

I. Introduction

Vibrations of mechanical systems are generally characterized by low frequencies and low amplitudes; hence these systems could be suitably controlled by means of passive control systems, where external energy isn't required [1, 2]. Nevertheless, some industrial applications show a vibrating behavior at low frequencies but characterized quite high amplitudes; in this cases the passive control techniques show their own limits in term of performances. Moreover, besides a vibration control, it is sometimes needed a motion control too, for example in order to control the trim of a machine. In these cases, more complex control techniques should be used, as the active vibration control techniques. This paper deals with the mechatronic design of an active device for both the control of vibration and the trim's regulation. In particular, the design concerns a 3 dof actuated device which controls vibrations and trim of a platform. The design of the device has been developed according to a typical mechatronic approach [3, 4]. As a matter of fact, for an optimal design of the system, a synergistic interaction between three main parts is needed: the purely mechanical system, the drive system, the control system. For the set-up of the control system a detailed model of the device has been developed, identifying some of the parameters by means of experimental tests. After the design phase, several experimental tests have been performed, in order to evaluate the performances of the control strategy chosen.

Paolo Righettini, Roberto Strada, Riccardo Riva
University of Bergamo - Department of Engineering and Applied Sciences
Italy

II. System's description

As already mentioned, the device has been designed according to a functional mechatronic approach; as first step, a set of vibration levels to be controlled, and a set of reference trajectories have been defined. The device has a cartesian structure; it has three degrees of freedom realized by means of three orthogonal linear axes, hence they are completely uncoupled. The system is driven by brushless motors; the transformation from rotary to linear motion is achieved by means of ball screws and linear guides. As shown in Fig. 1 and Fig. 2, the device is composed of:

- Lower base: part connected to the vibrations source.
- Upper base: part where the vibration isolation and motion control are performed.
- Sensors: three accelerometers for the measurement of the accelerations along axis x, y, z directions (see Fig. 1).
- Actuators: axis x, y, z are driven by three brushless motors.

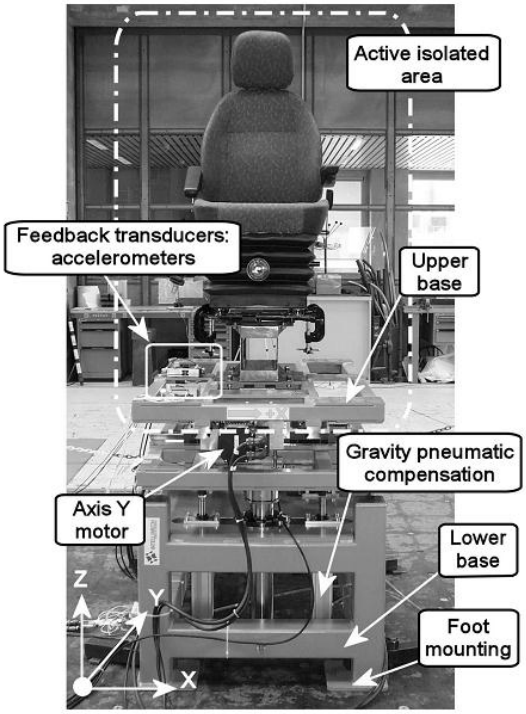

Figure 1. Device for active vibration and motion control

Proc. of the Second Intl. Conf. on Advances In Civil, Structural and Mechanical Engineering- CSM 2014.

ISBN: 978-1-63248-054-5 doi: 10.15224/ 978-1-63248-054-5-114

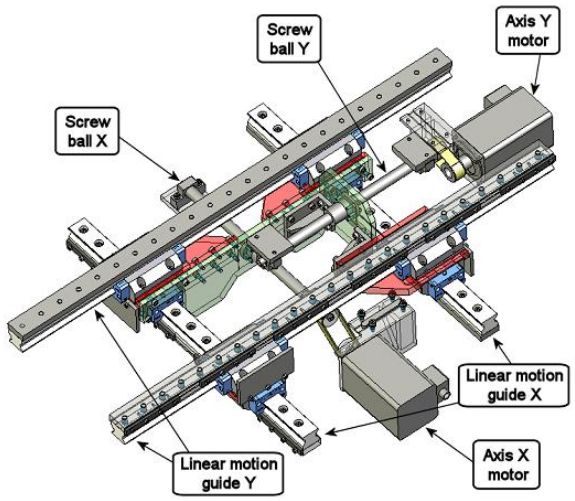

Figure 2. Details on x and y transmissions

As far as axes z is concerned, it has to balance also the gravitational forces due to the weight of the upper base. In order to be able to choose a motor similar in size to the one of axis x and y, pneumatic actuators connected to a pressurized tank have been used to balance the gravitational forces. As already mentioned, the axes has been designed to be completely uncoupled; such design choice allows a simpler implementation of the control system: the 3 dofs system is considered as three 1 dof systems. The dynamic modeling of the device and the experimental characterization tests have been developed on each axis at a time.

III. System's model

The general form of the equation of motion for the whole system can be written as:

$$\mathbf{M\ddot{\Theta} + C\dot{\Theta} + K\Theta = F} \tag{1}$$

where:

$\mathbf{\Theta}$ is a 6x1 array containing the motors and ball screw rotations for the three axes (see Fig. 3).

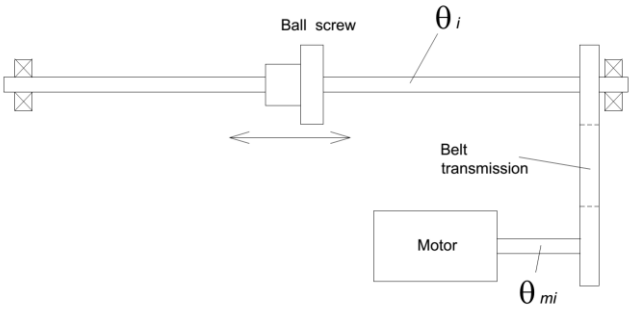

Figure 3. Axes configuration sketch

M is the mass matrix, **C** is the damping matrix, **K** is the stiffness matrix and **F** is the array of external actions.

The stiffness matrix is mainly associated to the belt stiffness, while the damping coefficient have been experimentally evaluated, as shown in the following sections.

Being the three axis completely uncoupled, mass, damping and stiffness matrices have the following shape:

$$\mathbf{M} = \begin{bmatrix} \mathbf{M1} & & \mathbf{0} \\ & \mathbf{M2} & \\ \mathbf{0} & & \mathbf{M3} \end{bmatrix} \tag{2}$$

$$\mathbf{C} = \begin{bmatrix} \mathbf{C1} & & \mathbf{0} \\ & \mathbf{C2} & \\ \mathbf{0} & & \mathbf{C3} \end{bmatrix} \tag{3}$$

$$\mathbf{K} = \begin{bmatrix} \mathbf{K1} & & \mathbf{0} \\ & \mathbf{K2} & \\ \mathbf{0} & & \mathbf{K3} \end{bmatrix} \tag{4}$$

where **Mi**, **Ci**, **Ki** are 2x2 matrices related to *i*th axis.

In particular:

$$\mathbf{Mi} = \begin{bmatrix} J_i^* & 0 \\ 0 & J_{im}^* \end{bmatrix}, \mathbf{Ci} = \begin{bmatrix} c_i & 0 \\ 0 & 0 \end{bmatrix}, \mathbf{Ki} = \begin{bmatrix} k_{t,ii} & k_{t,iim} \\ k_{t,imi} & k_{t,imim} \end{bmatrix} \tag{5}$$

where:

J^*_i is the total reflected moment of inertia on ball screw axis;

J^*_{im} is the total reflected moment of inertia on motor axis;

c_i is the total reflected damping coefficient on the ball screw axis

$k_{t,ii}$, $k_{t,iim}$, $k_{t,imi}$, $k_{t,imim}$ are the torsional stiffness coefficients related to the belt transmission stiffness.

As far as the array of external action is concerned, it has the following shape:

$$\mathbf{F} = [\mathbf{F1} \quad \mathbf{F2} \quad \mathbf{F3}]^T \tag{6}$$

where **Fi** is the following 2x1 array:

$$\mathbf{Fi} = [T_{di} \quad T_{mi}]^T \tag{7}$$

where T_{di} is the disturbance torque acting on the ball screw, while T_{mi} is the motor torque, which is the control variable used to drive each axis.

In order to properly define the control system, it is useful to write the systems model equation in variable state form. Starting from the dynamic equation of the generic axis *i*:

$$\mathbf{M_i\ddot{\Theta}_i + C_i\dot{\Theta}_i + K_i\Theta_i = F_i} \tag{8}$$

where $\mathbf{\Theta_i}=[\vartheta_i \quad \vartheta_{mi}]^T$, and introducing the array of state variables:

Proc. of the Second Intl. Conf. on Advances In Civil, Structural and Mechanical Engineering- CSM 2014.

ISBN: 978-1-63248-054-5 doi: 10.15224/ 978-1-63248-054-5-114

$$\mathbf{V_i} = [\ddot{\Theta}_i \ \dot{\Theta}_i]^T \quad (9)$$

it is possible to write:

$$\dot{\mathbf{V}}_i = \begin{bmatrix} -\mathbf{M}_i^{-1}\mathbf{C}_i & -\mathbf{M}_i^{-1}\mathbf{K}_i \\ \mathbf{I} & \mathbf{0} \end{bmatrix} \mathbf{V}_i + \begin{bmatrix} 0 \\ 1 \\ 0 \\ 0 \end{bmatrix} T_{mi} + \begin{bmatrix} 1 \\ 0 \\ 0 \\ 0 \end{bmatrix} T_{di} \quad (10)$$

where T_{mi} is the driving action related to axis *i*.

IV. Experimental characterization of the system

At the aim to set-up a detailed model of the system and to be able to develop a proper control system, an experimental characterization of the unknown system's parameters has been performed. In particular, the attention has been focused on the friction, the damping coefficient, and on the natural frequencies of the system mainly related to the belt transmission stiffness.

A. *Friction identification*

The evaluation of dynamic friction allows to determine the viscous damping coefficients of the axes. The dynamic friction experimental tests have been performed moving the linear axes at constant speed and measuring the relevant motors' torques needed. the results of this procedure is summarized in Fig. 4 where the viscous friction torque of axis *x* is represented. Being the behavior of the motors' torques linear, the viscous damping (c_1, c_2, c_3) of the three axes can be evaluated as the slope of the relevant curves.

Other tests have been performed in order to identify the static friction torques needed to make the axes move from rest. The test on each axis has been carried out increasing the relevant motor's supply current until the axis starts moving. As an example, Fig. 5 show the results for axis *x* and *y*. Known both the dynamic friction torque and the static one, it is possible to draw the Stribeck curves [5, 6]. As an example, Fig. 6 shows the Stribeck curve for axis *x*.The definition of the Stribeck curves allow to design a control system where the non linearities and the viscous forces effect are compensated by means of proper control actions. As shown in Fig. 6, the Stribeck isn't symmetical with respect to ordinate axis; this might be expressive of a bad alignment between linear guides and ball screws. Hence, the system's model and the control strategy take into account also this unexpected characteristic.

B. *Natural frequencies*

The natural frequencies of the system have been determined by means of a dynamometric hammer giving an impulsive excitation to each axis and measuring the signal of the relevant accelerometer. Fig. 7 and Fig. 8 shows, as an example, the acceleration time history and the relevant spectrum.

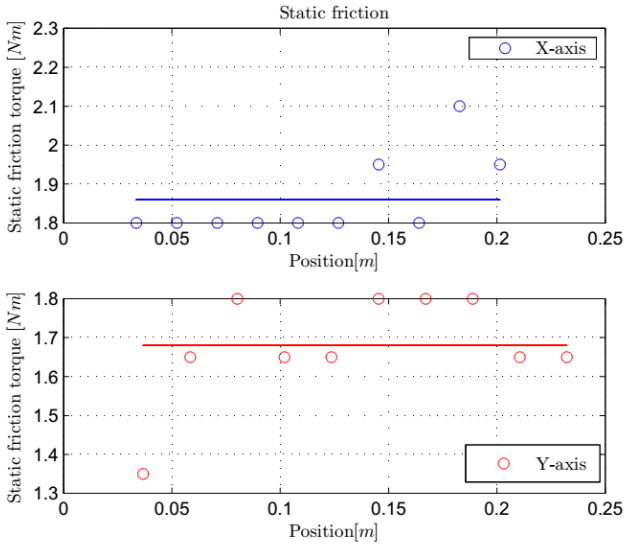

Figure 4. Static friction identification for *x* and *y* axis

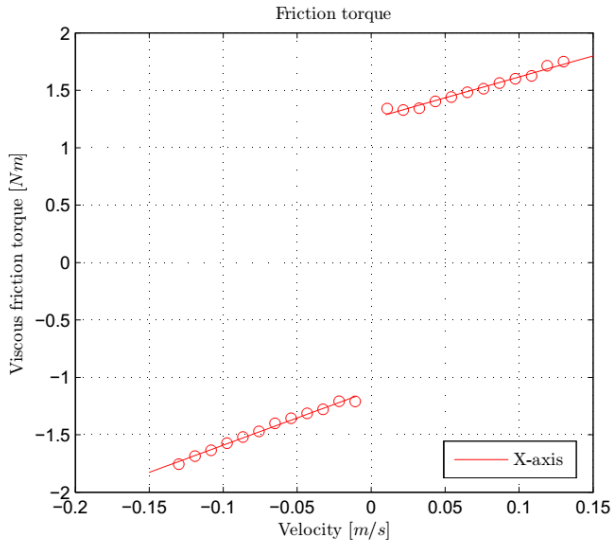

Figure 5. Viscous friction characterization for *x* axis

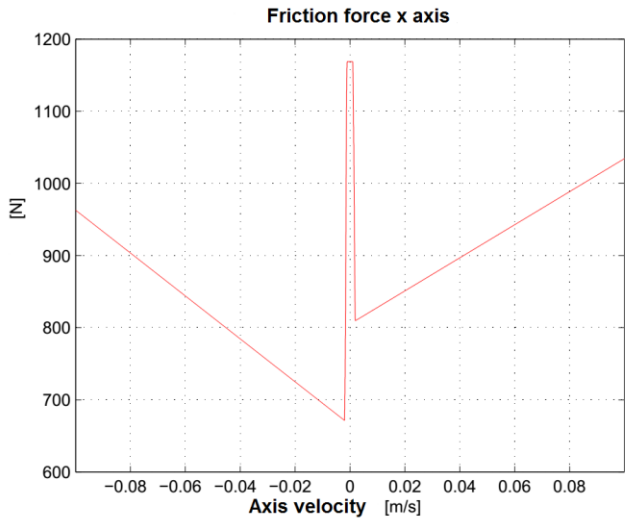

Figure 6. Stribeck curve for *x* axis

Proc. of the Second Intl. Conf. on Advances In Civil, Structural and Mechanical Engineering- CSM 2014.

ISBN: 978-1-63248-054-5 doi: 10.15224/ 978-1-63248-054-5-114

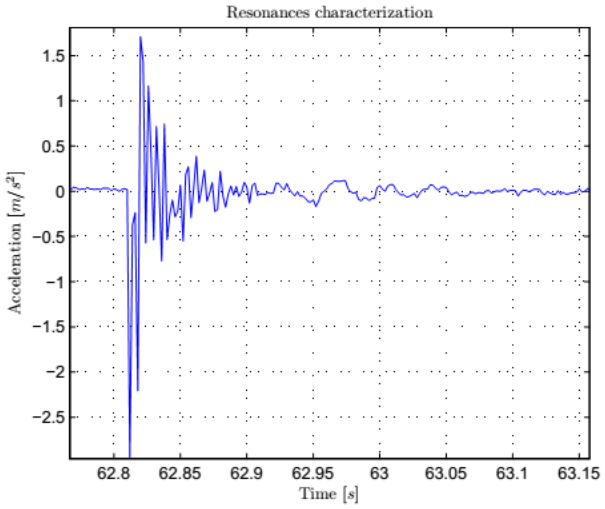

Figure 10. Acceleration time history for *x* axis

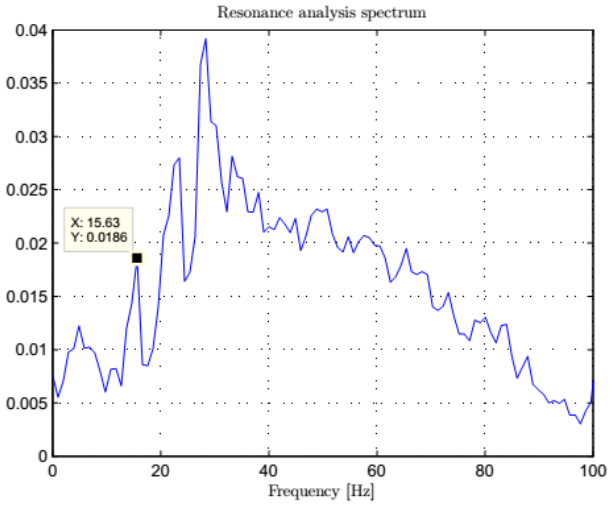

Figure 7. Resonance frequencies identification for *x* axis

On the basis of the determined resonance frequencies, the attention has been focused on the prevalent one. Being the masses of the system known, fro that frequency the stiffness coefficients due to the belt transmission and to other un-modeled stiffnesses have been identified.

On the basis of the parameters identified, the Bode diagram of the open loop system can be drawn (Fig. 9).

v. Control system design

The control system is composed of three different contributions (see Fig. 10), each one giving a specific control action: vibration control, friction compensation, position control. The aim of the control system is to set to zero the acceleration of the upper base against the vibration of the lower base, modeled as the disturb *d*. Being the axes of the device completely uncoupled, the regulators gains are tuned considering the system composed of three 1 dof systems.

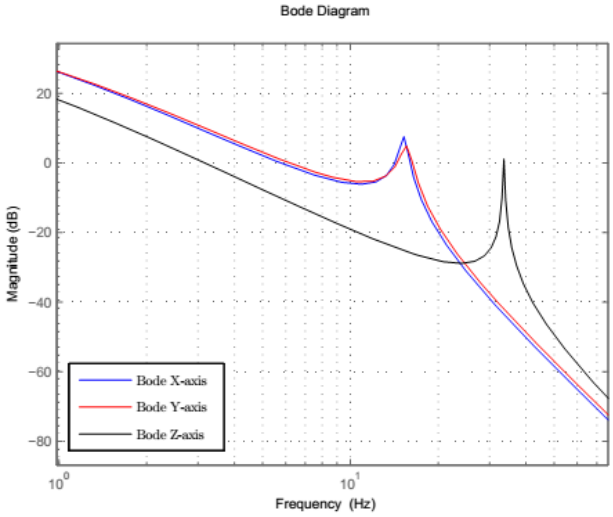

Figure 9. Bode diagram of the open loop system

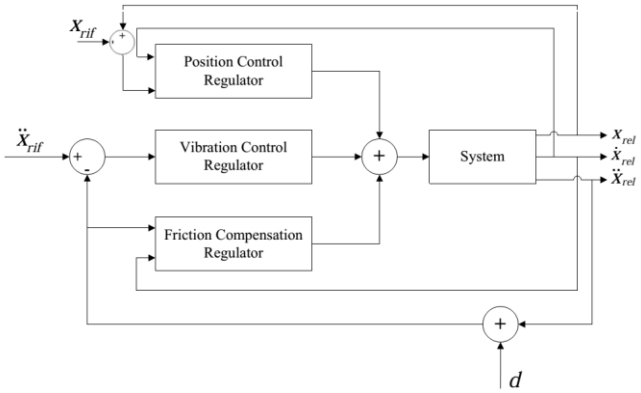

Figure 8. Control system configuration

A. *Vibration control*

The active vibration control system uses as feedback signal the measurement of the accelerometers located on the upper basis. According to those signals, the motors introduce torques (command actions) in order to keep the upper base accelerations zero. The command actions are determined according to the following relation:

$$\mathbf{u} = -\begin{bmatrix} g_x & 0 & 0 \\ 0 & g_y & 0 \\ 0 & 0 & g_z \end{bmatrix} \ddot{\mathbf{X}}_{\mathbf{abs}} \qquad (11)$$

where $\mathbf{u}=[T_{mx}\ T_{my}\ T_{mz}]^T$ is the command action array containing the motors torques, g_x, g_y, g_z are the regulator gains, $\ddot{\mathbf{X}}_{\mathbf{abs}}$ is the array of the absolute accelerations along the direction of each axis. Being the axes completely uncoupled, the gains are determined separately for each axis. As far as the regulator is concerned, it has the following shape:

$$R(s) = \mu \frac{1 + s/\omega_z}{1 + s/\omega_p} \qquad (12)$$

The choice of the frequencies of the pole and the zero is accomplished by analyzing the disturb sensitivity function. Fig. 11 shows the Bode diagram of the sensitivity function

Proc. of the Second Intl. Conf. on Advances In Civil, Structural and Mechanical Engineering- CSM 2014.

ISBN: 978-1-63248-054-5 doi: 10.15224/ 978-1-63248-054-5-114

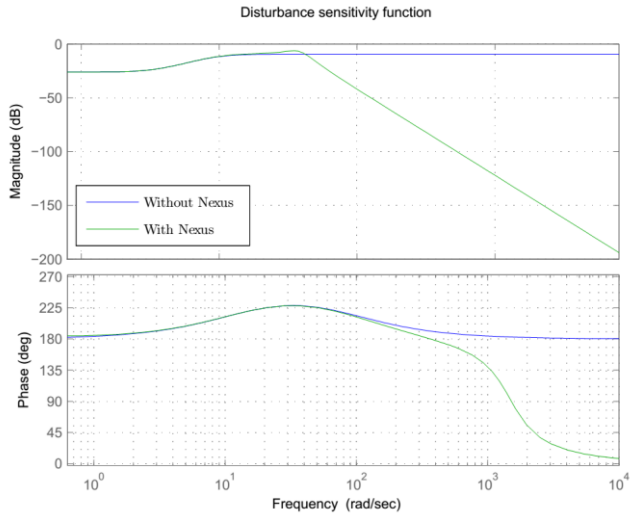

Figure 11. Disturbance sensitivity function

with or without taking into account the transfer function of the signal conditioning device. This transfer function has been determined by proper experimental tests. As well known, the pole has an integral action and it has been chose so to reduce the influence of the disturb; in particular it has been chosen near to the origin with a frequency of *2 Hz*. The zero is chosen in order to limit the bandwidth, hence to limit the range within vibrations are controlled. The chosen zero frequency is 20 Hz. Fig. 12 represents the closed loop transfer function of the system where the input is the acceleration of the lower base and the output is the upper base acceleration. As previously mentioned and showed in Fig. 8 the system is characterized by a natural frequency; we have decided to attenuate the effect of the most influent frequency by menas of a notch filter. The final tuning of the regulator has been done by means of simulations performed in Matlab/Simulink environment, taking into consideration also some typical aspects of real control systems as signal quantization, measurements disturbances, digital filters, commands saturation.

B. *Friction compensation*

In order to take into account also the friction phenomena inside the control system, a specific control action has been introduced. This action allows to compensate for the presence of friction both dynamic and static. The control algorithm is based on the Stribeck curves experimentally determined; according to the position and velocity of the axis, the motor gives an additional torque which allows friction compensation.

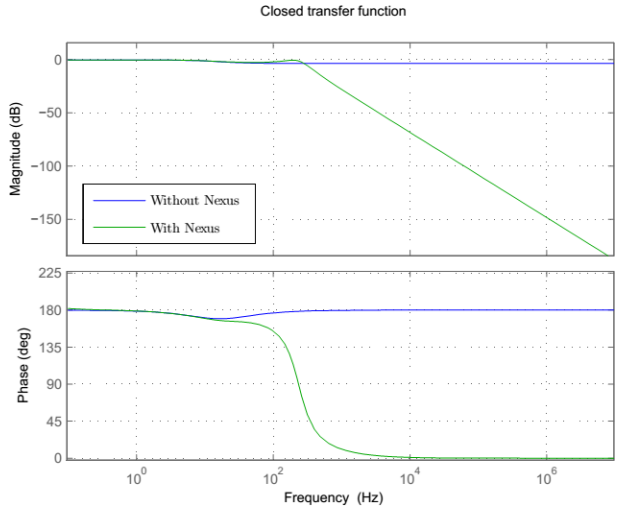

Figure 12. Closed loop transfer function

C. *Position control*

The position control regulator has been introduced for two main reasons: during the vibration control it prevent axes drift towards the end-strokes, and it allows motion control and vibration control at the same time. The motion control is realized by means of poles placement technique. The choice of the poles must guarantee to properly follow the set-point $\mathbf{X_{rif}}$ (see Fig. 10), without to influence the vibration control system. Hence the poles frequencies must be lower than the minimum frequency of vibration to be controlled. In particular, for x and y axes a 2 Hz frequency and a 1.1 damping coefficient; for z axis a 1 Hz frequency has been chosen.

VI. Experimental tests

The system realized is characterized by the following parameters:

- Upper base dimensions: 4 m x 4 m.
- Maximum axes stroke: 200 mm.
- Maximum forces: 500 N horizontal, 600kN vertical.
- Maximum acceleration: 45 m/s^2 horizontal, 50 m/s^2 vertical.
- Frequency range 0-10 Hz.

The performances of the system have been evaluated with some preliminary experimental tests carried on by means of a 3 dofs shaking table on which the device has been fixed in order to apply known accelerations to its lower base. In particular, the results reported refer to the following tests:

1. Sinusoidal excitation of the lower base with an acceleration along *y* axis with a frequency of 5 Hz and an amplitude of 4 m/s^2, keeping the upper base in a fixed position (Fig. 13 and Fig. 14).
2. Sinusoidal excitation of the lower base with an acceleration along *z* axis with a frequency of 9 Hz and an amplitude of 4 m/s^2, keeping the upper base in a fixed position (Fig. 15 and Fig. 16).
3. Sinusoidal excitation of the lower base with an acceleration along *x* axis with a frequency of 5 Hz and an amplitude of 4 m/s^2, making the upper base follow a circular trajectory of 75 mm radius in the plane *xz* (Fig. 17 and Fig. 18).
4. Sweep excitation along y axis: frequency range 3-10 Hz and amplitude 6 m/s^2 (fig. 19).

Proc. of the Second Intl. Conf. on Advances In Civil, Structural and Mechanical Engineering- CSM 2014.

ISBN: 978-1-63248-054-5 doi: 10.15224/ 978-1-63248-054-5-114

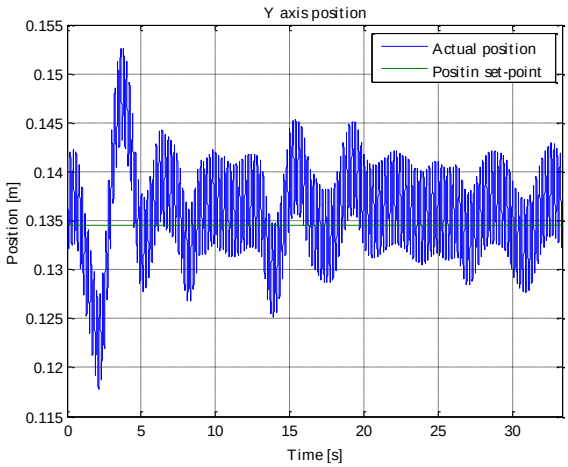

Figure 13. Actual and set-point position for test 1

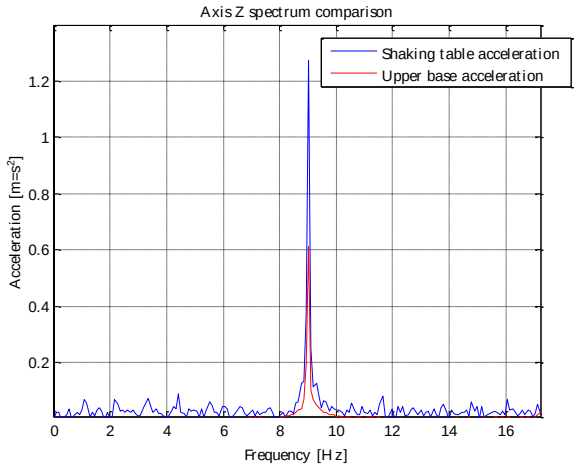

Figure 16. Acceleration spectrum for test 2

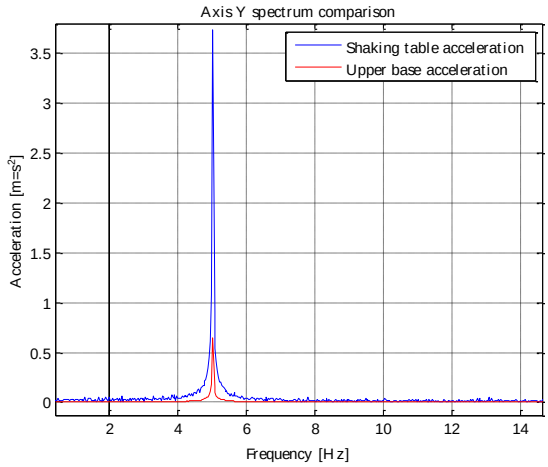

Figure 14. Acceleration spectrum for test 1

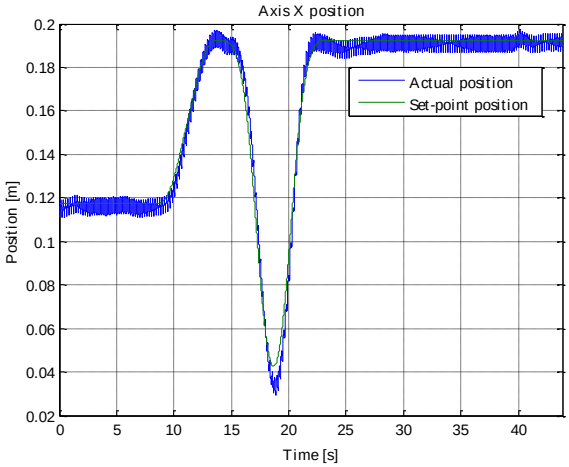

Figure 17. Actual and set-point position for test 3

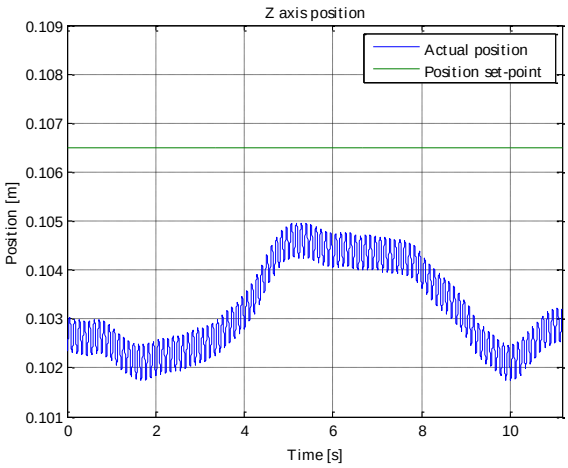

Figure 15. Actual and set-point position for test 2

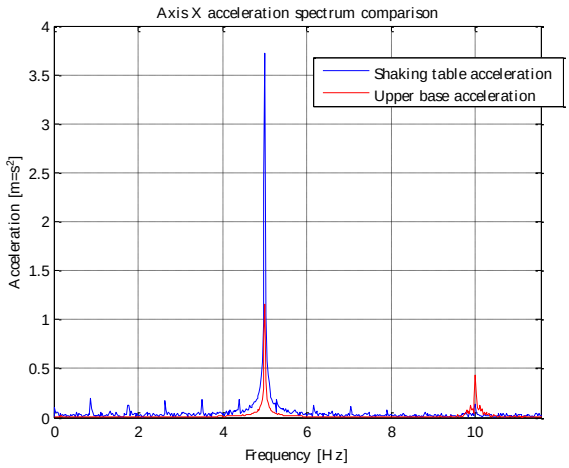

Figure 18. Acceleration spectrum for test 3

Proc. of the Second Intl. Conf. on Advances In Civil, Structural and Mechanical Engineering- CSM 2014.

ISBN: 978-1-63248-054-5 doi: 10.15224/ 978-1-63248-054-5-114

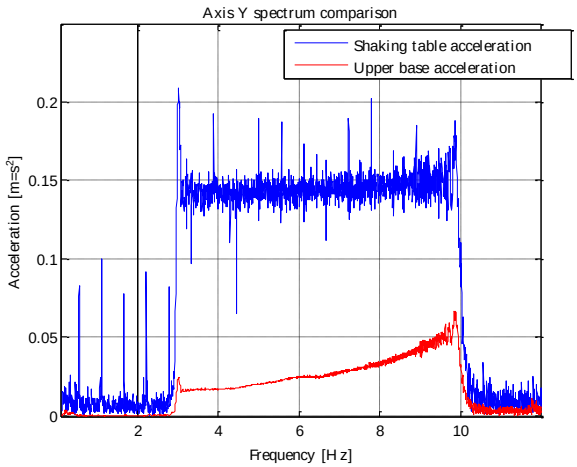

Figure 19. Acceleration spectrum for test 4

Fig. 13 to Fig. 16 show that for a sinusoidal excitation of the base along an axis, the acceleration of the upper base is significantly lower than the excitation itself. Moreover, the systems is able to keep the desired position with a very small error.

Similar remarks can be made for Fig. 17 and Fig. 18; in particular, Fig. 17 shows that the upper base follow the desired position with a very small error, and fig. 18 shows that the acceleration of the upper base is about four times lower than the excitation one.

Finally, Fig. 19 shows that the performance of the system is good in all the range of interesting frequencies; as a matter of fact, at maximum frequency of 10 Hz, the acceleration of the upper base is three times lower than the excitation one.

VII. Conclusions

In this paper, the design of a mechatronic device for both active control of vibrations and motion control have been presented. The design phase followed a typical mechatronic approach where a synergistic interaction between three main parts is needed. For the set-up of the control system a detailed model of the device has been developed, identifying some of the parameters by means of experimental tests.

After the design phase, the device has been realized and some preliminary experimental tests have been carried on. The tests show that the system has good performances, being able to attenuate the accelerations coming from the lower base up to 10 Hz with amplitudes up to 4 m/s^2. The tests show also that the system, in the mean time, can also properly follow a trajectory.

However, other experimental tests are already planned to deeply investigate the performances of the system, in order to achieve will be carried on to fully validate the device.

References

[1] E.I. Rivin, “Passive Vibration Isolation”, Asme press, 2003

[2] Y, Ishida, “Recent development of the passive vibration control method”, Mechanical Systems and Signal Processing, Volume 29, May 2012, Pages 2-18

[3] C. W. De Silva. “Mechatronics – an integrated approach”, CRC Press - Taylor & Francis Group, 2005.

[4] W. Bolton. “Mechatronics: electronic control systems in mechanical and electrical engineering”. Addison Wesley, Prentice Hall, 2004.

[5] Yong-Sub Yi, et al “Dynamic analysis of a linear motion guide having rolling elements for precision positioning devices”, Journal of Mechanical Science and Technology 22 (2008) 50~60

[6] C.L. Chen, M.J. Jang, K.C. Lin “Modeling and high-precision control of a ball-screw-driven stage”, Precision Engineering 28 (2004) 483–495.

About Authors:

Paolo Righettini is Associate Professor of Applied Mechanics. Research interests: Design of complex mechatronic systems, dynamics and vibration control of mechanical systems

Roberto Strada is Assistant Professor of Applied Mechanics. Research interests: mechatronics, electro-hydraulic driving systems, dynamics of mechanical systems

Riccardo Riva is Full Professor of Applied Mechanics. Research interests: Mechanical vibrations, Dynamics of mechanical systems, Mechanical transmission systems.